

Microbial Sulfur Isotope Fractionation in the Chicxulub Hydrothermal System

David A. Kring,¹ Martin J. Whitehouse,² and Martin Schmieler^{1,3}

Abstract

Target lithologies and post-impact hydrothermal mineral assemblages in a new 1.3 km deep core from the peak ring of the Chicxulub impact crater indicate sulfate reduction was a potential energy source for a microbial ecosystem (Kring *et al.*, 2020). That sulfate was metabolized is confirmed here by microscopic pyrite framboids with $\delta^{34}\text{S}$ values of -5 to -35 ‰ and $\Delta\text{S}_{\text{sulfate-sulfide}}$ values between pyrite and source sulfate of 25 to 54 ‰, which are indicative of biologic fractionation rather than inorganic fractionation processes. These data indicate the Chicxulub impact crater and its hydrothermal system hosted a subsurface microbial community in porous permeable niches within the crater's peak ring. Key Words: Origin of life—Hydrothermal—Impact crater—Chicxulub. *Astrobiology* 21, 103–114.

1. Introduction

THE ~180 KM DIAMETER Chicxulub impact crater is the best-preserved peak-ring basin on Earth. Evidence of an extensive impact-generated hydrothermal system in the Chicxulub crater emerged with the initial studies of the samples used to link the impact crater to the K-T boundary mass extinction event (Kring and Boynton, 1992). Crater lithologies were crosscut by veins of anhydrite and silica, and the rocks' primary mineralogy and textures were overprinted with hydrothermal mineral assemblages. Soon thereafter similar alteration was described at other impact craters (notably by Naumov, 1993, 1996, 1999; McCarville and Crossey, 1996), suggesting hydrothermal activity is a common consequence of impact heating in hydrous planetary crust.

Such systems would have been particularly prevalent during the Hadean when Earth was being bombarded by late accreting asteroids and comets. Some of the largest of those impacts should have vaporized seas (Sleep *et al.*, 1989), making conditions untenable for life at the surface. Based on observations at Chicxulub (Kring and Boynton, 1992), the idea emerged that those same impact events produced vast subsurface hydrothermal systems that were potential crucibles for prebiotic chemistry and habitats for the early evolution of life (Kring 2000a, 2000b, 2003), that is, the impact origin of life hypothesis. The end of

that period of impact bombardment coincided with what may be the earliest evidence of life (*e.g.*, Mojzsis and Harrison, 2000; *cf.* Whitehouse and Fedo, 2007), although it was not certain (and remains uncertain) whether life truly emerged at that time or was of a type capable of surviving the bombardment (Maher and Stevenson, 1988; Chyba, 1993). Analyses of ribosomal RNA made in the same decade indicated the earliest organisms on Earth were thermophilic (Woese *et al.*, 1990; Pace 1991, 1997). It seemed plausible that life originated in an impact crater (Kring, 2000a, 2000b, 2003).

To test that concept, studies of Chicxulub, our best proxy of large Hadean impact craters, continued. Chicxulub is the only large peak-ring basin that is still intact and provides an opportunity to study the remnants of an impact-generated hydrothermal system, from depth up to and including the venting surface environment, similar to those that may have existed earlier in Earth's history. Thermal evolution models of that and other hydrothermal systems indicated they were long-lived and produced significant volumes of porous, permeable rock suitable for thermophilic organisms (Abramov and Kring, 2004, 2005, 2007). The International Continental Scientific Drilling Program (ICDP) drilled into Chicxulub in 2001–2002, recovering core in the moat between the crater rim and peak ring. Traces of a hydrothermal system were found in ~100 m of impactites (Ames *et al.*, 2004; Hecht

¹Lunar and Planetary Institute, Universities Space Research Association, Houston, Texas, USA.

²Department of Geosciences, Swedish Museum of Natural History, Stockholm, Sweden.

³HNU–Neu-Ulm University of Applied Sciences, Neu-Ulm, Germany.

et al., 2004; Kring *et al.*, 2004; Lüders and Rickers, 2004; Rowe *et al.*, 2004; Zürcher and Kring, 2004; Zürcher *et al.*, 2005; Nelson *et al.*, 2012), augmenting the findings from the borehole that provided evidence of the structure's impact origin (Kring and Boynton, 1992) and producing an evolutionary sequence of the hydrothermal system with time and depth in that portion of the crater (Zürcher and Kring, 2004). Those two boreholes, Yucatán-6 (Y-6) and Yaxcopoil-1 (Yax-1), are located ~ 10 and ~ 25 km beyond the peak ring (Fig. 1), respectively, indicating hydrothermal activity was not a local phenomenon but rather part of an extensive system. Furthermore, it became increasingly clear (Cockell, 2006) that that type of system had the potential to host life.

To explore the hydrothermal system further, in 2016 the International Ocean Discovery Program (IODP) and ICDP sponsored Expedition 364, drilling a borehole into the peak ring of the Chicxulub crater where model results (Abramov and Kring, 2007) suggested hydrothermal activity may have been extensive. The expedition's petrologic analyses of the recovered core verified hydrothermal activity occurred with initially high temperatures in excess of 300°C (Kring *et al.*, 2017a, 2020). As the system cooled, high-temperature hydrothermal assemblages were crosscut by veins of, and pervasively overprinted by, lower-temperature mineral assemblages that precipitated as temperatures decreased from $\sim 250^{\circ}\text{C}$ to an ambient post-impact temperature of $\sim 25^{\circ}\text{C}$ in the upper peak ring breccias (Abramov and Kring, 2007), before the peak ring was buried to its current depth of

~ 617 m below the seafloor (Morgan *et al.*, 2016). One of the lower-temperature mineral assemblages is composed of analcime and dachiardite-Na (hereafter dachiardite), sometimes with heulandite and calcite, and FeS_2 framboids.

An important goal of Expedition 364 was to assess the biological potential of that hydrothermal system. Petrologic examination of the core (Kring *et al.*, 2020; Simpson *et al.*, 2020) indicated there were sharp redox gradients that may have been suitable for microbial reduction and oxidation processes. A potential by-product of microbial activity is sulfide, such as FeS_2 framboids (*e.g.*, Kohn *et al.*, 1998; Popa *et al.*, 2004; MacLean *et al.*, 2008; *cf.* Wilkin and Barnes, 1997). Here we examine the sulfur isotopic signature of sulfide minerals that exist in lower-temperature and, thus, biologically compatible mineral assemblages, to determine whether sulfate reduction was a biologically mitigated process (*e.g.*, as in Canfield and Thamdrup, 1994; Kohn *et al.*, 1998; Popa *et al.*, 2004; Shen and Buick, 2004; Sim *et al.*, 2011).

2. Methods

2.1. Petrography

Rock textures, crosscutting relationships, and initial mineral identification were made with a petrographic microscope at the Lunar and Planetary Institute. Electron microprobe analyses of phase chemical compositions and additional Raman spectroscopy were made at the Johnson Space Center. The procedures are the same as those used for other core samples (Kring *et al.*, 2020, where they are described in detail).

2.2. Measuring $\delta^{34}\text{S}$ and $\delta^{13}\text{C}$

Microscale sulfur and carbon stable isotope measurements were performed with a CAMECA IMS1280 large-geometry ion microprobe at the Swedish Museum of Natural History (NordSIMS facility). Operation of the instrument in multi-collector mode, with the secondary magnet field regulated to high stability by using an NMR field sensor, was common to both methods. Instrument settings for $\delta^{34}\text{S}$ in pyrite broadly follow those described in the work of Whitehouse (2013). A primary beam of $^{133}\text{Cs}^+$ ions with 20 kV incident energy and beam current of either ~ 500 pA for the framboidal samples or ~ 1 nA for the massive pyrites was critically (Gaussian) focused with, respectively, a 5 or 10 μm raster applied during analysis to homogenize the beam profile. Secondary ion signals of ^{32}S and ^{34}S were measured by using two Faraday cups operating at a common mass resolution ($M/\Delta M$) of 2460. Analyses of $\delta^{13}\text{C}$ in calcite used similar primary beam tuning, but with a slightly larger beam current (2.5 nA) and a 10 μm raster. Simultaneous detection of ^{12}C and ^{13}C signals was made in a Faraday cup at $M/\Delta M$ of 2460 and an ion counting electron multiplier at $M/\Delta M$ of 4000, sufficient to resolve ^{13}C from $^{12}\text{C}^1\text{H}$. For both methods, a normal incidence electron gun was used for charge compensation. All presputter, beam centering, and data acquisition steps were automated in the run definition. Sample measurements were bracketed by reference pyrite (S0302A, $\delta^{34}\text{S}_{\text{V-CDT}} = 0.0$ ‰) and calcite (S0161; $\delta^{13}\text{C}_{\text{V-PDB}} = -2.0$ ‰) measurements to correct for instrumental mass bias (both reference materials kindly provided by R. Stern, University of Alberta; V-CDT and V-PDB refer to the reference values for Vienna Canyon

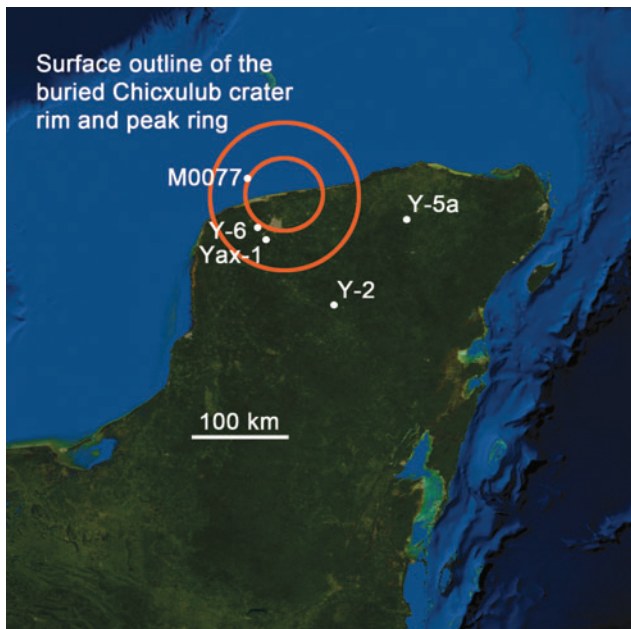


FIG. 1. Location of the Chicxulub peak-ring crater beneath the northern edge of the Yucatán Peninsula, México. Samples analyzed in the current study were recovered from the International Ocean Discovery Program and International Continental Scientific Drilling Program Expedition 364 Site M0077 borehole. Other samples described in the paper were recovered from boreholes Yucatán-2 (Y-2), Yucatán-5a (Y-5a), Yucatán-6 (Y-6), and Yaxcopoil-1 (Yax-1). Background: NASA image produced by MODIS satellite observations in October 2004.

Diablo Troilite and Vienna Pee Dee Belemnite, respectively). Within-run uncertainties were propagated together with the standard deviation obtained from the relevant reference materials during the analytical session to yield the overall reported uncertainty (Table 1).

3. Results

Samples of the Chicxulub peak ring were recovered from 617.33 meters below the seafloor (mbsf) to 1334.68 mbsf at Site M0077 (Morgan *et al.*, 2016, 2017; Kring *et al.*, 2017b). The uppermost part of the peak ring is composed of ~104 m of breccia with impact melt fragments (reworked suevite, Unit

2 of the logged core; Morgan *et al.*, 2017). That material overlies ~25 m of clast-poor and clast-rich impact melt rock (Unit 3). Those impactites cover felsic basement rocks. For the current study, three samples were selected from the porous, permeable breccia sequence, and a fourth sample was selected from the bottom of the core. The deepest sample (0077-297R-1, 93 to 95 cm; 1313.92 mbsf) is a polymict breccia with solidified impact melt fragments (suevite) that occurs within granitoid rocks of the peak-ring, 697 m below the contact between the upper peak-ring lithologies and an overlying siltstone. The interval is hydrothermally altered with secondary garnet (andradite), epidote, pyrite, chalcocopyrite, galena, calcite, and clay minerals. This suevite unit does not contain sedimentary clasts, which are evident in upper peak ring suevites (Kring *et al.*, 2017c). The sulfide analyzed here has a rhombohedral habit and occurs along the margin of secondary sparitic calcite (Fig. 2).

The other three samples are from the upper portion of the peak-ring sequence. The deepest of those (0077-63R-2, 69.5 to 72 cm; 685.47 mbsf) is from Subunit 2B, a relatively well-sorted, suevite that occurs 68 m beneath the top of the peak-ring lithologies. The breccia contains fragments of the crystalline basement and overlying carbonate platform sedimentary rocks. The breccia is hydrothermally altered with secondary silica, pyrite, chalcocopyrite, other Fe-Co-Ni sulfides, barite, clay minerals, calcite, dachiardite, and analcime. The sample contains both irregular-shaped FeS₂ and framboidal FeS₂ (Fig. 2), the latter along an open network of channels lined with dachiardite and other zeolites.

Two samples are from Subunit 2A. One of the samples (0077-46R-1, 46 to 52 cm; 635 mbsf) is a suevite that occurs 29.52 m above the bottom of Subunit 2A, which is separated from 2B by an erosional contact. Subunit 2A has a similar matrix and clast content as 2B, but is less coarse than the underlying suevite 2B. The sample interval is hydrothermally altered with secondary silica, pyrite, chalcocopyrite, calcite, and clay minerals. Pyrite occurs as framboids concentrated along the walls of a subvertical vent channel (Fig. 2). The sample was ~18 m beneath the top of the peak-ring lithologies. The other sample from Subunit 2A (0077-40R-2, 105 to 107 cm; 618.72 mbsf) is a relatively well-sorted suevite near the top of Subunit 2A and 1.39 m beneath the top of the peak-ring lithologies. The interval is hydrothermally altered with secondary pyrite, chalcocopyrite, calcite, and clay minerals (Kring *et al.*, 2020). The sulfide minerals are isolated and aggregate rhombohedral crystals (Fig. 2). Local cockscomb-textured aggregates suggest those Fe-sulfides may include marcasite (Schmieder *et al.*, 2017a).

The suevite samples contain several sulfide phases: chalcocopyrite (CuFeS₂), galena (PbS), pentlandite ((Fe,Ni)₉S₈), pyrite (FeS₂), sphalerite (ZnFeS), and villamaninite ((Cu,Ni,Co,Fe)S₂) (Kring *et al.*, 2020). Here we focus on those crystals with FeS₂ compositions, because they may be a by-product of biogenic processes (*e.g.*, Popa *et al.*, 2004). We refer to the crystals with FeS₂ compositions in samples 0077-46R-1 and 0077-63R-2 as pyrite rather than its polymorph marcasite, based on the framboid morphology. Moreover, Raman spectra confirm FeS₂ is pyrite in all four samples, including cockscomb-textured crystal aggregates.

The coarse-grained rhombohedral pyrite in 0077-40R-2 and 0077-297R-1 coexists with calcite (CaCO₃). Finer-grained

TABLE 1. ISOTOPE DATA FOR SULFIDE AND COEXISTING CALCITE CRYSTALS

Sample	$\delta^{34}S_{V-CDT}$	$\pm \text{‰}$	$\delta^{13}C_{V-PDB}$	$\pm \text{‰}$
40-2-105-107	-17.23	0.05	0.30	0.30
	-17.23	0.05	0.30	0.30
	-13.22	0.05	-1.85	0.30
	-14.16	0.05	-2.10	0.29
	-11.84	0.05	-1.69	0.30
	-13.82	0.05	-1.34	0.30
	-9.21	0.05	-1.16	0.29
46-1-46-52	-27.82	0.10	0.93	0.31
	-26.90	0.16	0.11	0.33
	-29.68	0.08	0.93	0.33
	-22.65	0.07	0.51	0.33
	-30.38	0.07	-0.05	0.31
	-24.73	0.07	-0.52	0.31
	-23.53	0.06	-1.88	0.36
	-20.57	0.07	-1.28	0.35
	-35.91	0.09	0.24	0.31
	-29.58	0.09	1.09	0.31
	-28.78	0.07	-1.96	0.31
	-24.11	0.11	-7.59	0.30
	-23.62	0.09		
-33.14	0.11			
63-2-69.5-72	-15.99	0.06		
	-15.89	0.07		
	-14.92	0.07		
	-17.99	0.08		
	-17.62	0.08		
	-20.96	0.07		
	-6.22	0.08		
	-18.68	0.08		
	-18.15	0.07		
	-6.15	0.07		
	-17.35	0.06		
	-17.83	0.08		
	-16.71	0.07		
	-18.43	0.10		
	-21.57	0.07		
-8.81	0.06			
297-1-93-95	-2.85	0.05	-2.32	0.30
	-3.03	0.05	-7.61	0.29
	-1.86	0.05	-4.10	0.29
	-3.10	0.05	-5.47	0.30
	-2.23	0.05	-5.97	0.30
			-7.06	0.32

Calcite did not coexist with pyrite in 63-2-69.5-72. A table with standard values and other analytical values is in a permanently curated data repository (<http://hdl.handle.net/20.500.11753/1700>).

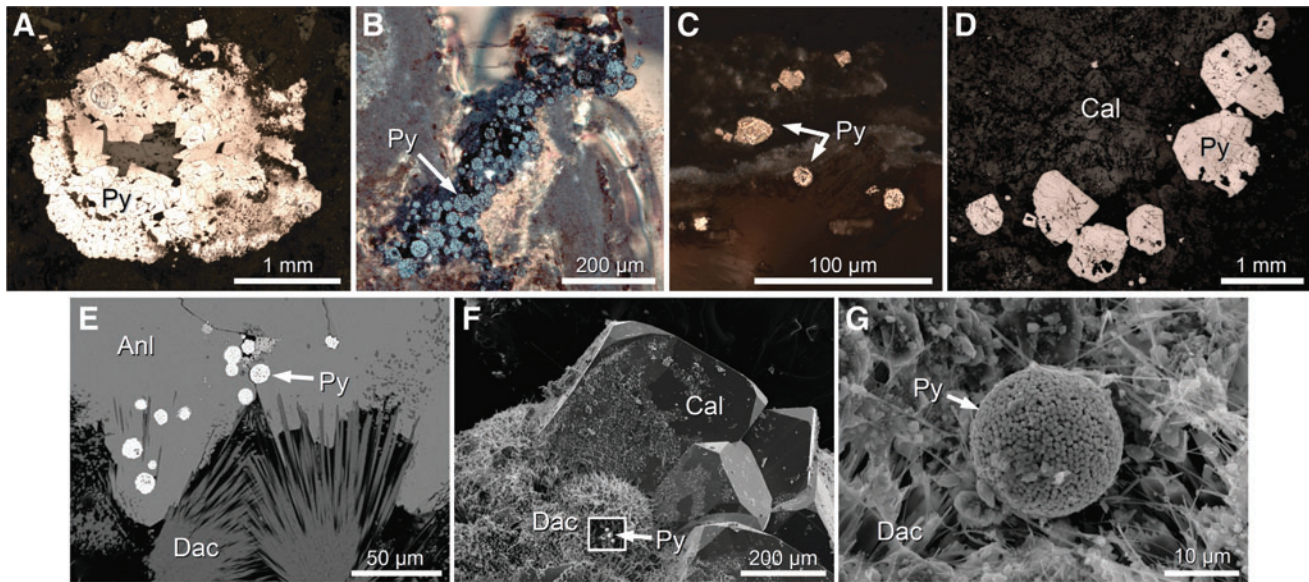


FIG. 2. Images of sulfide. Regions analyzed for sulfur isotopes in (A) 0077-40R-2, (B) 0077-46R-1, (C) 0077-63R-2, and (D) 0077-297R-1. (E) Pyrite framboids within analcime, 0077-63R-1. (F) Pyrite framboid adjacent to calcite, 0077-63R-1. (G) Pyrite framboid exposed by abrasion within analcime and with potential biofilm, 63R-1. Optical microscopic images (A–D), backscattered electron image (E), and secondary electron images (F, G). Labeled bars provide scale of each image. Anl = analcime; Cal = calcite; Dac = dachiardite; Py = pyrite.

pyrite framboids in 0077-46R-1 and 0077-63R-2 coexist with the zeolite minerals analcime ($\text{NaAlSi}_2\text{O}_6 \cdot \text{H}_2\text{O}$), dachiardite ($\text{Na}_{10}\text{Al}_{10}\text{Si}_{38}\text{O}_{96} \cdot 25\text{H}_2\text{O}$) (Fig. 2), and heulandite ($(\text{Na,Ca})_{2-3}\text{Al}_3(\text{Al,Si})_2\text{Si}_{13}\text{O}_{36} \cdot 12\text{H}_2\text{O}$). Analcime grew as blocky, orthorhombic, equidimensional, trapezohedron crystals and occasionally as sprays of thinner crystals, while dachiardite grew as thin crystal sprays that formed botryoidal masses. The habits of the zeolite crystals indicate they grew into pore spaces within the suevite. They also fill pore spaces in large multi-centimeter-wide swaths through the rock (see Fig. 2 in Kring *et al.*, 2020). Pyrite framboids are enclosed within analcime and dachiardite, indicating that the framboids grew with the zeolites and that the zeolites continued to grow after the framboids precipitated.

Millimeter-sized rhombohedral pyrite crystals at the bottom and top of the core have $\delta^{34}\text{S}$ values of -1.86 ± 0.05 to -3.10 ± 0.05 ‰ and -9.21 ± 0.05 to -17.23 ± 0.05 ‰, respectively (Fig. 3). Coexisting calcite has $\delta^{13}\text{C}$ values of 0.30 ± 0.30 to -7.61 ± 0.29 ‰. The 10–20 μm diameter pyrite framboids have very different sulfur isotope values. Framboids ~ 68 m beneath the top of the peak ring (sample 0077-63R-2, 69.5 to 72 cm; 685.47 mbsf) have $\delta^{34}\text{S}$ values of -5 to -22.5 ‰. Framboids ~ 18 m beneath the top of the peak ring (sample 0077-46R-1, 46 to 52 cm; 635 mbsf) have $\delta^{34}\text{S}$ values of -20 to -36 ‰ (Fig. 3). Co-existing calcite has $\delta^{13}\text{C}$ values of 0.93 ± 0.33 to -7.59 ± 0.30 ‰.

4. Discussion

The ~ 180 km diameter Chicxulub impact crater was produced by an impacting asteroid with ~ 100 million megatons of kinetic energy, which is ~ 6 million times more energetic than the largest nuclear explosion test conducted by the United States (*e.g.*, Kring, 1993). The impact event uplifted relatively warm crustal rocks from a depth of 8–

10 km (Morgan *et al.*, 2016) and produced 10^4 to 10^5 km³ of impact melt (Kring, 1995), heating subsurface water and producing a crater-wide hydrothermal system. Soon after the crater was excavated, it was flooded by the sea, covering the peak ring in the location of the Expedition 364 borehole by as much as 600 m of water (Gulick *et al.*, 2019). The pressure at the top of any venting hydrothermal system at that depth was ~ 6000 kPa (880 psi or 60 atm), assuming a seawater density of 1.03 g/cm³. The system would have been biologically sterile during the high-temperature phase, but as temperatures approached 100°C , porous, permeable niches in the impactites had the potential to host microbial life. Conditions ($\sim 50^\circ\text{C}$ to 120°C) suitable for thermophilic life may have persisted for ≥ 2 million years (Kring *et al.*, 2020), initially in the outer regions of the crater, far from the central melt sheet, and then in areas closer to the crater center as the melt sheet cooled (see Fig. 3 of Abramov and Kring, 2007, for an evolutionary sequence with 25°C to 100°C temperature contours in time steps at 4 thousand, 20 thousand, 200 thousand, and 2 million years after impact).

Water feeding the system was dominated by groundwater (Zurcher *et al.*, 2005; Abramov and Kring, 2007) flowing through a carbonate platform sequence with sulfate strata and through impact breccias that contained fragments of sulfate rocks. Those waters, entering the hydrothermal system, were circulated upward carrying dissolved sulfate and partially vented at the seafloor-seawater interface. Although the bulk of the water was a basinal brine (Zurcher *et al.*, 2005), some drawdown of sulfate-bearing seawater was possible (Abramov and Kring, 2007), producing mixing zones.

Sulfate (anhydrite) clasts (Fig. 4) were observed in the Y-6 polymict impact breccias (Hildebrand *et al.*, 1991; Kring *et al.*, 1991; Kring and Boynton, 1992; Sharpton *et al.*, 1996; Claeys *et al.*, 2003), ~ 65 km SSE of Site M0077. Anhydrite was also found in bedrock beneath the Yax-1 impactites,

FIG. 3. Sulfur isotope compositions for sulfide from four hydrothermally altered core samples recovered by IODP-ICDP Expedition 364 in order of relative depth in the peak ring. Forty-one sulfide analyses were made in suevite within peak ring granitoid rocks (0077-297R-1-93-95, pink squares) and three overlying suevitic breccias (0077-63R-2-69.5-72, yellow squares; 0077-46R-1-46-52, green squares; 0077-40R-2-105-107, blue squares). Analytical uncertainty is smaller than the sizes of symbols. Expedition 364 sulfur isotopes in 22 samples of post-impact sediments (open squares) and their stratigraphic age are from Schaefer *et al.* (2020). For comparison, analyses of sulfate samples in bedrock of the northern Yucatán (Claypool *et al.*, 1980; Koeberl 1993), in Chicxulub ejecta on the Yucatán (Koeberl 1993), and in two previous core samples (Y-6 and Yax-1) recovered from the crater (Strauss and Deutsch, 2003) are provided (gray squares). Sulfide isotope compositions (‰, V-CDT) of the pyrite framboids are extremely fractionated from those of target sulfate compositions.

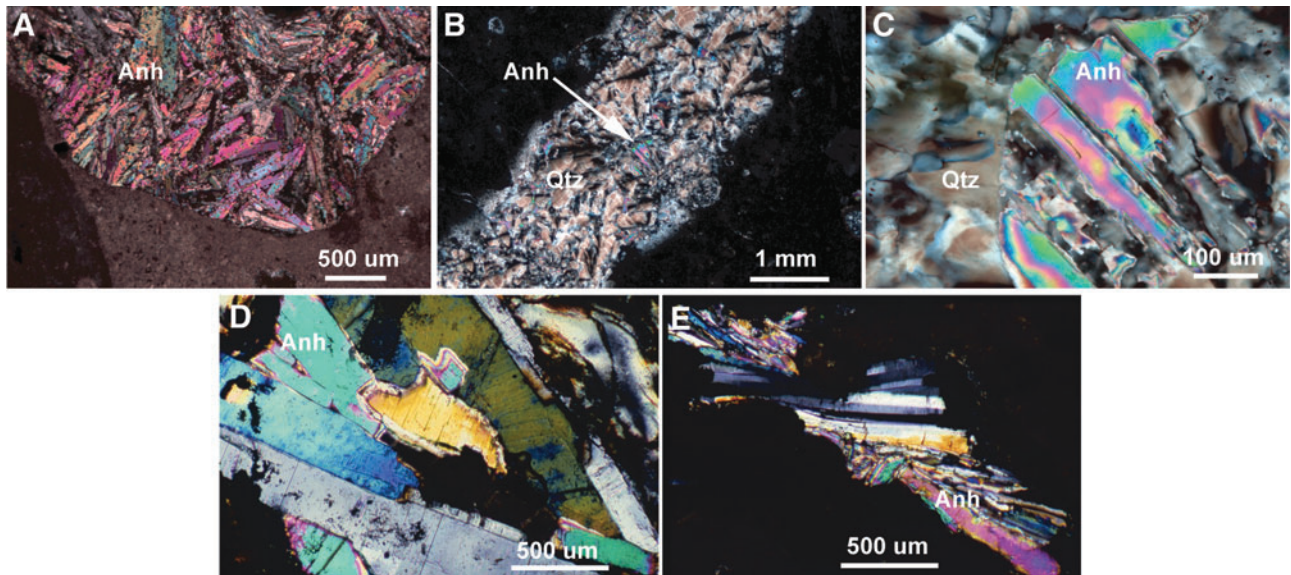
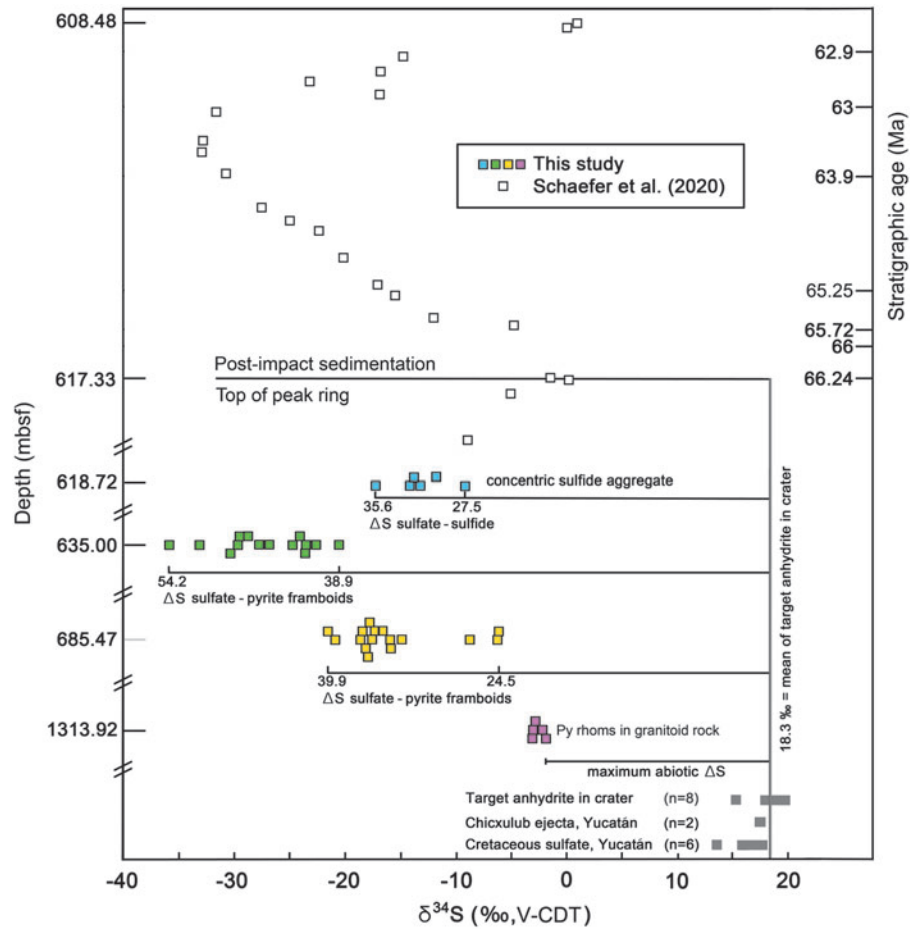


FIG. 4. Images of sulfate (anhydrite). (A) Clast of target bedrock anhydrite (Anh) in polymict impact breccia, Y6-N14. (B) Quartz (Qtz)-anhydrite vein in polymict impact breccia, Y6-N19. (C) Close-up of anhydrite in quartz-anhydrite vein, Y6-N19. (D-E) Cavity-filling blooms or sprays of secondary anhydrite filling vesicles in altered impact melt fragments in polymict impact breccia, Y6-N14. Optical microscope images with crossed-nicols. Labeled bars provide scale of each image.

although no clasts were observed in the impact breccias (e.g., Kring *et al.*, 2004), ~80 km SSE of Site M0077. It is not yet clear if sulfate was heterogeneously distributed in the target rock sequence or if the variation observed in impactites is a product of impact excavation, deposition, and modification processes (Kring, 2005). That sulfate was incorporated into hydrothermal fluids is explicitly shown by anhydrite (CaSO₄) veins in Y-6 core samples (Kring and Boynton, 1992; Schmieder *et al.* 2019), anhydrite veins in Yax-1 core samples (Zurcher *et al.*, 2005), secondary anhydrite in Y-6 samples (Kring and Boynton, 1992), and secondary barite (BaSO₄) in an M0077 core sample with pyrite framboids (0077-63R-2) and in samples ~3, 12, and 32 m deeper in the core (Kring *et al.*, 2020). Sulfate was initially incorporated into hydrothermal fluids at temperatures $\geq 270^\circ\text{C}$ based on Ti-in-quartz geothermometry of quartz–Ti-magnetite–anhydrite veins (Schmieder *et al.*, 2019), whereas anhydrite also precipitated later at lower temperatures in voids within the breccia (Fig. 4; see also Claeys *et al.*, 2003), particularly within cavities of once-glassy melt fragments that were altered to smectite.

Bedrock sulfate in northern Yucatán has $\delta^{34}\text{S}$ values of 13.7–17.7 ‰ (Claypool *et al.*, 1980; Koeberl, 1993). Sulfate clasts in Chicxulub ejecta deposited on the Yucatán peninsula, recovered in boreholes Yucatán-2 and Yucatán-5a, have $\delta^{34}\text{S}$ values of 17.5 and 17.6 ‰ (Koeberl, 1993). Sulfate clasts recovered in two previous boreholes into the crater (Y-6 and Yax-1) have $\delta^{34}\text{S}$ values of 18.0–19.8 ‰ (Strauss and Deutsch, 2003). The mean of samples from within the crater is 18.3 ‰, representing the groundwater reservoir and overlying seawater values. The maximum abiogenic $\Delta\text{S}_{\text{sulfate-sulfide}}$ is ~20 ‰ (Machel, 2001; Popa *et al.*, 2004), which is about that seen in rhombohedral pyrite at the base of the borehole (Fig. 3). An abiogenic origin for the rhombohedral pyrite is also consistent with the absence of an unambiguous biogenic carbon isotope signature in the associated calcite.

In contrast, the $\delta^{34}\text{S}$ values of the pyrite framboids in the suevite are much lower, producing $\Delta\text{S}_{\text{sulfate-sulfide}}$ of ~25 to 54 ‰, greatly exceeding abiogenic fractionation. Such large $\Delta\text{S}_{\text{sulfate-sulfide}}$ values are signatures of microbial reduction of sulfate (e.g., Popa *et al.*, 2004). Similar sulfate-sulfide fractionation was observed in the smaller, ~24 km diameter Haughton crater (Canada) where sulfate also occurs in the target bedrock (Parnell *et al.*, 2010) and ~40 km diameter Rochechouart crater (France) where sulfate is inferred to have been extracted from seawater (Simpson *et al.*, 2017). We also note that pyrite framboids, albeit without sulfur isotope data, were observed in hydrothermally-altered rocks of the ~52 km diameter Siljan crater (Sweden) in association with carbonaceous matter with biogenic-like and microbial-like features (Hode *et al.*, 2009).

While samples 0077-46R-1 and 0077-63R-2 were initially 18 and 68 m beneath the seafloor, respectively, by the time the hydrothermal system cooled to temperatures suitable for thermophilic microbes, 1–10 m of marine sediment blanketed the peak ring, depending on the cooling rate of the hydrothermal system (Kring *et al.*, 2020). Thus, sulfate reduction to produce framboidal pyrite was occurring to depths of 20–80 m below seafloor vents.

Textures indicate sulfate reduction occurred in the hydrothermal system, rather than under normal, low bottom water, shallow sedimentary temperatures after the hydro-

thermal system ceased operating. The pyrite framboids in 0077-46R-1 occur along the zoned walls of a vent channel, and the pyrite framboids in 0077-63R-2 occur along the zoned walls of a network of channels lined with hydrothermal dachiardite. The framboids are not distributed homogeneously or diffusively through the rock as a consequence of equilibrium pore water precipitation beneath a seawater-sediment interface. Nor are the framboids distributed in horizontal layers reflective of a kinetically controlled process parallel to the seawater-sediment interface.

As noted above, pyrite framboids grew amid the zeolites dachiardite and analcime, sometimes in association with heulandite and calcite. In natural hydrothermal environments, analcime and heulandite are generally produced at temperatures between 25°C and 100°C (Iijima, 1980), although they and dachiardite are stable at higher temperatures (Coombs *et al.*, 1959; Liou, 1971; Ueda *et al.* 1980; Bargar and Beeson, 1984; Bargar *et al.*, 1987). Heulandite may follow analcime precipitation as temperatures fall below 100–120°C (Mehegan *et al.*, 1982; Utada 2001). At Yellowstone, heulandite was observed at hydrothermal temperatures of ~40°C and ~80°C at depths of 17 and 30 m (Bargar and Beeson, 1984). Pyrite framboids in association with heulandite, analcime, and calcite (Prol-Ledesma *et al.* 2002) have precipitated from submarine vents with fluid temperatures of 85–87°C (Núñez-Cornú *et al.* 2000; Alfonso *et al.*, 2005). Elsewhere, analcime and heulandite, with pyrite, calcite, and other phases, may have been a product of hydrothermal alteration between 60°C and 70°C (Keith and Staples, 1985). Because the pyrite framboids in those samples and in our sample 0077-46R-1 are associated with calcite, we note that clumped isotope analyses of calcite deposited immediately on top of the breccias analyzed here record hydrothermal temperatures of 70°C (Bralower *et al.*, 2020).

Modern strains of thermophilic sulfate-reducing bacteria exist at those temperatures at hydrothermal vents and hot springs. For example, *Thermodesulfobacterium hydrogenophilum* (50–80°C; Jeanthon *et al.* 2002) and *Desulfobacteriales* (40°C and 70°C; Dhillon *et al.* 2003) were isolated from hydrothermal vents in the Gulf of California's Guaymas Basin, with sulfate reduction peaking between 60°C and 90°C (Kallmeyer and Boetius, 2004). *Thermodesulfobacterium geofontis* (70–90°C; Hamilton-Brehm *et al.*, 2013) and *Thermodesulfobacterium yellowstonii* (40–70°C; Henry *et al.*, 1994) were isolated from a thermal vent and pool, respectively, in Yellowstone National Park. Other examples associated with hydrothermal vents, subsurface geothermal waters, and hot oil field water include *Thermodesulfator atlanticus* (55°C and 75°C; Alain *et al.* 2010), *Desulfothermus okinawensis* (35–60°C; Nunoura *et al.* 2007), *Desulfotomaculum* and *Thermanaeromanas* (50–80°C; Kaksonen *et al.* 2006), and *Thermodesulforhabdus norvegicus* (44–74°C; Beeder *et al.*, 1995). Sulfate reduction is a metabolic path utilized by archaea, too. For example, *Archaeoglobus fulgidus* (peak sulfate reduction rate at 82–84°C; Mitchell *et al.*, 2009; see also Stetter *et al.*, 1987, and Khelifi *et al.*, 2010, 2014) was isolated from an active seafloor vent in Italy; and *Archaeoglobus profundus* (growing at temperatures up to 90°C; Burggraf *et al.*, 1990) was isolated from a submarine hydrothermal vent in the Guaymas Basin.

The observed biological sulfur isotope fractionation in our Chicxulub samples required an energy source, or

electron donors, for sulfate reduction (*e.g.*, Smith and Klug, 1981; Jeanthon *et al.*, 2002; Alazard *et al.*, 2003; Kallmeyer and Boetius, 2004; Finke *et al.*, 2007; Liamleam and An-nachhatre, 2007; Cao *et al.*, 2014). Potential electron donors in the Chicxulub system are hydrocarbons that are observed in a porous and permeable impact-brecciated zone within target carbonate beneath hydrothermally altered impactites in the Yax-1 core (Kring *et al.*, 2004). Mobilization and transport of those hydrocarbons are indicated by hydrocarbon-bearing fractures and hydrocarbon-filled pores observed at the base of the Yax-1 impactite sequence and an isotopic signature of hydrocarbons detected in an overlying unit of impact breccias (Zurcher *et al.*, 2005). Hydrocarbons were also detected in fluid inclusions in those upper peak-ring breccias and, when the hydrocarbons were entrained in hydrothermal fluids during the initial higher-temperature phase of the system, appear to have cracked to form ethane and propane (Lüders and Rickers, 2004). Hydrogen may have also been available when impact glass and other Chicxulub crater lithologies were altered (Christou and Bach, 2019), including mafic intrusions in the uplifted peak ring of the crater that contain decomposed olivine (Gulick *et al.*, 2017; Schmieder *et al.*, 2017b). Carbon sources may have included CO₂ from dissolving carbonate and, at the top of the sequence, potentially wood and charcoal deposited at the top of the impactite sequence in the Expedition 364 core (Bralower *et al.*, 2020).

Calcite carbon isotope values ($\delta^{13}\text{C}$) in sample 0077-46R-1 are 0.93 ± 0.33 to -7.59 ± 0.30 ‰. If hydrocarbons were the electron donor, the observed values imply carbonate precipitation was not contemporaneous with pyrite formation or, perhaps more likely, that the isotopes in the calcite are dominated by the limestone and limestone-derived carbonate beneath and throughout the breccia sequence, which have $\delta^{13}\text{C}$ values of 0–2.9 ‰ (Lüders *et al.*, 2003) and may have averaged 2 ‰ (Zurcher *et al.* 2005). A bulk $\delta^{13}\text{C}$ value of -7.2 ‰ in a Yaxcopoil-1 impact breccia was likewise interpreted to reflect mixing of isotopic contributions from a methane (CH₄)-bearing fluid and the carbonate reservoir of Chicxulub (Zurcher *et al.*, 2005). Isotopic mixing of that type is observed in a modern hydrothermal sulfate-reducing system in the Gulf of California's Guaymas Basin, in that case producing intermediate $\delta^{13}\text{C}$ values of -11.7 ± 1.6 ‰ from organic carbon values of -21.4 ‰ that mixed with marine limestone values of 0 ‰ (Peter and Shanks, 1992). We note that it is also possible that hydrocarbons, while present, were partially to wholly supplanted by other electron donors, such as H₂, which would not have driven $\delta^{13}\text{C}$ to strongly negative values. Some sulfate-reducing thermophiles utilize electrons from mixtures of hydrocarbons and hydrogen (Beeder *et al.*, 1994; Henry *et al.*, 1994; Hamilton-Brehm *et al.*, 2013).

If we momentarily expand our view from the peak-ring location of the samples described here to the crater-wide hydrothermal system, we note that fluid chemistry will not be uniform, either in space or time. At a slightly greater distance from the crater center, in the Yaxcopoil-1 borehole, fluids were derived from basinal brines, with hydrocarbons, and had neutral to alkaline pH (Zurcher *et al.*, 2005). Conditions were not, however, static, as the hydrothermal system cooled through phases of Ca-Na metasomatism, K metasomatism, clay precipitation (*e.g.*, by the alteration of impact-generated glasses), and diagenesis (Zurcher and Kring, 2004). Interior to the peak ring, we envision a sep-

arate stream of fluids emanating from a ~3 km thick central melt sheet with a grossly andesitic composition produced by bulk melting of the crust (Kring and Boynton, 1992). The melt sheet would have thermally consumed and contact-metamorphosed bounding crystalline bedrock, releasing additional fluids that may have been carried upward along the inner walls of the peak ring and possibly through fractures created in uplifted target rock by the impact event. Near the top of the hydrothermal system, whether that be near the peak ring or over the central melt sheet, seawater may have been drawn down and created thermal and chemical mixing zones. Models of fluid flow and heat transport in the Chicxulub system that were calculated by using the computer code HYDROTHERM (Abramov and Kring, 2007) indicate the relative proportions of fluids from different regions of the crater, delivered to any one place in the crater, changed with time. Thus, boreholes drilled elsewhere in the crater may reveal other hydrothermal alteration patterns and metabolic strategies.

It is important to note that a diverse array of microbes was identified in enrichment experiments and with DNA extraction techniques within the site M0077 impactites (Cockell *et al.*, 2019). The organisms occur at depths where temperatures exceed 45°C (Gulick *et al.*, 2017) and are, thus, thermophilic. We cannot completely rule out the possibility that the sulfide framboids analyzed here were produced by this modern assemblage of organisms, but we favor their origin in the original, post-impact hydrothermal system for the following reasons.

First, the pyrite framboids are enclosed within analcime and dachiardite, not on the surfaces of existing fractures and pore spaces. Second, the framboids occur along the margins of a clay-rich vent channel produced soon after impact (*e.g.*, Fig. S5 of Kring *et al.*, 2020). Third, and perhaps more telling, evidence of sulfate reducers exists in sediments deposited on top of the peak ring within 4 million years of impact (Fig. 3). An excursion of $\delta^{34}\text{S}$ to -33 ‰ occurs in Paleocene sediments deposited on the peak ring ~2.5 million years after the impact (Schaefer *et al.*, 2020), about the same time a thermal evolution model (Abramov and Kring, 2007) indicates thermophilic temperatures should be prevalent in the hydrothermal system. That sulfur isotope signature may reflect sulfate reduction in the water column above the submerged peak ring (Schaefer *et al.*, 2020). It is also possible the sulfide carrying that fractionated isotopic signature was vented from the hydrothermal system onto the seafloor and, thus, may be reflective of a subsurface biome. In either case, sulfate-reducing organisms existed in the crater ~66 to 63 million years ago. Fourth, we also note that it is easier to introduce organisms to the system when it is only a few meters beneath the seafloor, rather than at some later time when the suevite is getting buried progressively deeper by post-impact sediments, which are now 617 m thick. For these reasons, we suggest the pyrite framboids capture sulfate reduction that occurred in the crater soon after its formation. This implies that sulfate reducers found in the core today are living remnants of a 66 million-year-old microbial colony that emerged after the Chicxulub impact event.

Sulfate reduction is a process utilized by microbial organisms since at least the Paleoproterozoic, when it produced strongly depleted $\delta^{34}\text{S}$ in pyrite embedded in barite from North Pole, Australia (Shen *et al.*, 2001). Likewise, Paleoproterozoic microbial sulfate reduction produced strongly depleted $\delta^{34}\text{S}$ in pyrite now found in the Barberton Greenstone

Belt, South Africa (Roerdink *et al.*, 2013), possibly due to drawdown of seawater sulfate (Roerdink *et al.*, 2016). Thermophilic sulfate-reducing organisms occur deep within the bacterial domain (*e.g.*, Henry *et al.*, 1994). Nonetheless, Hadean environmental chemistry (*e.g.*, Kasting, 2005; Russell and Arndt, 2005; Zahnle *et al.*, 2007, 2020; Arndt and Nisbet, 2012) may have precluded the availability of sulfate as an energy source. Yet hydrothermal systems in which other metabolic reactions are utilized remain an attractive site for the early evolution of life (*e.g.*, Woese *et al.*, 1990; Reysenbach and Shock, 2002; Schwartzman and Lineweaver, 2004; Ciccarelli *et al.*, 2006), where high temperatures facilitate key reactions (Stockbridge *et al.*, 2010; Wolfenden *et al.*, 2015), either at oceanic ridges and continental volcanoes (*e.g.*, Shock and Schulte, 1998; Nisbet and Sleep, 2001; Martin *et al.*, 2008; Shibuya *et al.*, 2016), continental hot springs (Deamer *et al.*, 2019; Damer and Deamer, 2020), or through carbonaceous sedimentary layers (Westall *et al.*, 2018). Here we suggest that hydrothermal systems were being produced by a global distribution of impact cratering events, affecting all crustal lithologies and thus providing many of the same attributes that made previously described hydrothermal environments attractive. Serpentinization, for example, which produces H₂ as an energy source, may have reasonably occurred in impact craters that penetrated mafic and ultramafic crust (Schulte *et al.*, 2006).

5. Conclusions

Sulfur isotope analyses of pyrite framboids in impact breccia from the Chicxulub crater indicate thermophilic colonies of sulfate-reducing organisms inhabited the porous, permeable rock beneath the floor of the crater and fed on sulfate transported through the rock via an impact-generated hydrothermal system. Similar sulfur isotope signatures in overlying sediments (Schaefer *et al.*, 2020) imply sulfate-reducing organisms persisted for at least 2.5 million years after impact, potentially in both the subsurface and in the water column above the crater floor. Thermophilic sulfate-reducing organisms that currently occur in the same rocks, now buried hundreds of meters beneath the seafloor, may be the living remnants of that ~66 to 63 million-year-old colony of microorganisms.

Studies of Chicxulub have, thus, demonstrated that large peak-ring and multi-ring basins have porous, permeable subsurface environments; that such impact craters host vast subsurface hydrothermal systems; and that those systems can host microbial ecosystems. In the case of 66 Ma Chicxulub, sulfur isotope fractionation, indicative of microbial sulfate reduction, occurred, which is similar to the metabolic pathway used as long ago as 3.52 Ga in the Paleoproterozoic. In the Hadean, other metabolic reactions may have dominated the energy yields required by life, but, we suggest, those reactions may have occurred in the same type of porous, permeable impact-generated hydrothermal system that existed in the Chicxulub crater.

Acknowledgments

This research utilized samples provided by the International Ocean Discovery Program and International Continental Scientific Drilling Program. The research was supported by the National Science Foundation (grant OCE-1736826). The authors thank their expedition colleagues and MARUM staff for

core recovery, core logging, and first-generation studies of core material, which made this second-generation study possible. We thank the LPI library staff, which provided additional help when normal access to previously published research was curtailed by the COVID-19 pandemic. This is LPI Contribution No. 2545. LPI is operated by USRA under a cooperative agreement with the Science Mission Directorate of the National Aeronautics and Space Administration. The NordSIMS facility is supported by Swedish Research Council infrastructure grant 2017-00671; this is NordSIMS contribution 655. We thank three anonymous reviewers, Associate Editor Tim Lyons, Editor-in-Chief Sherry L. Cady, and journal staff for their help to sharpen the science in the paper and for doing so in the midst of a health emergency.

References

- Abramov, O., and Kring, D.A. (2004) Numerical modeling of an impact-induced hydrothermal system at the Sudbury crater. *J Geophys Res* 109, doi:10.1029/2003JE002213.
- Abramov, O., and Kring, D.A. (2005) Impact-induced hydrothermal activity on early Mars. *J Geophys Res* 110, doi: 10.1029/2005JE002453.
- Abramov, O., and Kring, D.A. (2007) Numerical modeling of impact-induced hydrothermal activity at the Chicxulub crater. *Meteorit Planet Sci* 42:93–112.
- Alain, K., Postec, A., Grinsard, E., Lesongeur, F., Prieur, D., and Godfroy, A. (2010) *Thermodesulfator atlanticus* sp. nov., a thermophilic, chemolithoautotrophic, sulfate-reducing bacterium isolated from a Mid-Atlantic Ridge hydrothermal vent. *Int J Syst Evol Microbiol* 60:33–38.
- Alazard, D., Dukan, S., Urios, A., Verh e, F., Bouabida, N., Morel, F., Thomas, P., Garcia, J.-L., and Ollivier, B. (2003) *Desulfovibrio hydrothermalis* sp. nov., a novel sulfate-reducing bacterium isolated from hydrothermal vents. *Int J Syst Evol Microbiol* 53:173–178.
- Alfonso, P., Prol-Ledesma, R.M., Canet, C., Melgarejo, J.C., and Fallick, A.E. (2005) Isotopic evidence for biogenic precipitation as a principal mineralization process in coastal gasohydrothermal vents, Punta Mita, Mexico. *Chem Geol* 224:113–121.
- Ames, D.E., Kjarsgaard, I.M., Pope, K.E., Dressler, B., and Pilkington, M. (2004) Secondary alteration of the impactite and mineralization in the basal Tertiary sequence, Yaxcopoil-1, Chicxulub impact crater, Mexico. *Meteorit Planet Sci* 39: 1145–1168.
- Arndt, N.T., and Nisbet, E.G. (2012) Processes of the young Earth and the habitats of early life. *Annu Rev Earth Planet Sci* 40:521–549.
- Bargar, K.E., and Beeson, M.H. (1984) *Hydrothermal Alteration in Research Drill Hole Y-6, Upper Firehole River, Yellowstone National Park, Wyoming*. Professional Paper 1054-B, US Geological Survey, Reston, VA.
- Bargar, K.E., Erd, R.C., Keith, T.E.C., and Beeson, M.H. (1987) Dachardite from Yellowstone National Park, Wyoming. *Can Mineral* 25:475–483.
- Beeder, J., Nilsen, R.K., Rosnes, J.T., Torsvik, T., and Lien, T. (1994) *Archaeoglobus fulgidus* isolated from hot North Sea oil field waters. *Appl Environ Microbiol* 60:1227–1231.
- Beeder, J., Torsvik, T., and Lien, T. (1995) *Thermodesulforhabdus norvegicus* gen. nov., sp. nov., a novel thermophilic sulfate-reducing bacterium from oil field water. *Arch Microbiol* 164: 331–336.
- Bralower, T.J., Cosmidis, J., Fantle, M.S., Lowery, C.M., Passey, B.H., Gulick, S.P.S., Morgan, J.V., Vajda, V., Whalen,

- M.T., Wittmann, A., Artemieva, N., Farley, K., Goderis, S., Hajek, E., Kring, D.A., Lyons, S.L., Rasmussen, C., Sibert, E., Rodríguez Tovar, F.J., Turner-Walker, G., Zachos, J.C., Carte, J., Chen, S.A., Cockell, C., Coolen, M., Freeman, K.H., Garber, J., Gonzalez, M., Gray, J., Grice, K., Heaney, P.J., Jones, H.L., Schaefer, B., Smit, J., and Tikoo, S.M. (2020) The habitat of the nascent Chicxulub crater. *AGU Advances*, in press. doi: 10.1029/2020AV000208.
- Burggraf, S., Jannasch, H.W., Nicolaus, B., and Stetter, K.O. (1990) *Archaeoglobus profundus* sp. nov. represents a new species within the sulfate-reducing Archaeobacteria. *Syst Appl Microbiol* 13:24–28.
- Canfield, D.E., and Thamdrup, B. (1994) The production of ^{34}S -depleted sulfide during bacterial disproportionation of elemental sulfur. *Science* 266:1973–1975.
- Cao, H., Wang, Y., Lee, O.O., Zeng, Z., Shao, Z., and Qian, P.-Y. (2014) Microbial sulfur cycle in two hydrothermal chimneys on the Southwest Indian Ridge. *mBio* 5, doi:10.1128/mbio.00980-13.
- Christou, E.V., and Bach, W. (2019) Post-impact habitability at the Chicxulub crater [6100]. In *82nd Annual Meeting of the Meteoritical Society*, Lunar and Planetary Institute, Houston.
- Chyba, C.F. (1993) The violent environment of the origin of life: progress and uncertainties. *Geochim Cosmochim Acta* 57:3351–3358.
- Ciccarelli, F.D., Doerks, T., von Mering, C., Creevey, C.J., Snel, B., and Bork, P. (2006) Toward automatic reconstruction of a highly resolved tree of life. *Science* 311:1283–1287.
- Claeys, P., Heuschkel, S., Lounejeva-Baturina, E., Sanchez-Rubio, G., and Stöffler, D. (2003) The suevite of the Chicxulub impact crater. *Meteorit Planet Sci* 38:1299–1317.
- Claypool, G.E., Holser, W.T., Kaplan, I.R., Sakai, H., and Zak, I. (1980) The age curves of sulfur and oxygen isotopes in marine sulfate and their mutual interpretation. *Chem Geol* 28: 199–260.
- Cockell, C.S. (2006) The origin and emergence of life under impact bombardment. *Philos Trans R Soc Lond B Biol Sci* 361:1845–1856.
- Cockell, C.S., Coolen, M.J.L., Schaefer, B., Grice, K., Wuchter, C., and the IODP Expedition 364 Team. (2019) Microbial communities and impact enhanced habitats in the Chicxulub impact crater [abstract 316-3]. In *2019 Astrobiology Science Conference*, Seattle, WA.
- Coombs, D.S., Ellis, A.J., Fyfe, W.S., and Taylor, A.M. (1959) The zeolite facies, with comments on the interpretation of hydrothermal synthesis. *Geochim Cosmochim Acta* 17:53–107.
- Damer, B., and Deamer, D. (2020) The hot spring hypothesis for an origin of life. *Astrobiology* 20:1–24.
- Deamer, D., Damer, B., and Kompanichenko, V. (2019) Hydrothermal chemistry and the origin of cellular life. *Astrobiology* 19:1–15.
- Dhillon, A., Teske, A., Dillon, J., Stahl, D.A., and Sogin, M.L. (2003) Molecular characterization of sulfate-reducing bacteria in the Guaymas Basin. *Appl Environ Microbiol* 69:2765–2772.
- Finke, N., Vandieken, V., and Jørgensen, B.B. (2007) Acetate, lactate, propionate, and isobutyrate as electron donors for iron and sulfate reduction in Arctic marine sediments, Svalbard. *FEMS Microbiol Ecol* 59:10–22.
- Gulick, S., Morgan, J., Mellett, C.L., Bralower, T., Chenot, E., Christeson, G., Claeys, P., Cockell, C., Coolen, M., Ferrière, G.C., Goto, K., Jones, H., Kring, D., Lofi, J., Lowery, C., Ocampo-Torres, R., Perez-Cruz, L., Pickersgill, A.E., Poelchau, M., Rae, A., Rasmussen, C., Rebolledo-Vieyra, M., Riller, U., Sato, H., Smit, J., Tikoo, S., Tomioka, N., Urrutia-Fucugauchi, J., Whalen, M., Wittmann, A., Yamaguchi, K., Xiao, L., and Zylberman, W. (2017) Site M0077: Upper Peak Ring. In *Proceedings of the International Ocean Discovery Program*, Vol. 364, International Ocean Discovery Program, College Station, TX, doi:10.14379/iodp.proc.364.106.2017.
- Gulick, S.P.S., Bralower, T.J., Ormö, J., Hall, B., Grice, K., Schaefer, B., Lyons, S., Freeman, K.H., Morgan, J.V., Artemieva, N., Kaskes, P., de Graaff, S.J., Whalen, M.T., Collins, G.S., Tikoo, S.M., Verhagen, C., Christeson, G.L., Claeys, P., Coolen, M.J.L., Goderis, S., Goto, K., Grieve, R.A.F., McCall, N., Osinski, G.R., Rae, A.S.P., Riller, U., Smit, J., Vajda, V., Wittmann, A., and the Expedition 364 Scientists. (2019) The first day of the Cenozoic. *Proc Natl Acad Sci USA* 39:19342–19351.
- Hamilton-Brehm, S.D., Gibson, R.A., Green, S.J., Hopmans, E.C., Schouten, S., van der Meer, M.T.J., Shields, J.P., Damsté, J.S.S., and Elkins, J.G. (2013) *Thermodesulfobacterium geofontis* sp. nov., a hyperthermophilic, sulfate-reducing bacterium isolated from Obsidian Pool, Yellowstone National Park. *Extremophiles* 17:251–263.
- Hecht, L., Wittmann, A., Schmitt, R.-T., and Stöffler, D. (2004) Composition of impact melt particles and the effects of post-impact alteration in suevitic rocks at the YAX-1 drill core, Chicxulub crater, Mexico. *Meteorit Planet Sci* 39:1169–1186.
- Henry, E.A., Devereux, R., Maki, J.S., Gilmour, C.C., Woese, C.R., Mandelco, L., Schauder, R., Remsen, C.C., and Mitchell, R. (1994) Characterization of a new thermophilic sulfate-reducing bacterium *Thermodesulfovibrio yellowstonii*, gen. nov. and sp. nov.: its phylogenetic relationship to *Thermodesulfobacterium commune* and their origins deep within the bacterial domain. *Arch Microbiol* 161:62–69.
- Hildebrand, A.R., Penfield, G.T., Kring, D.A., Pilkington, M., Camargo Z.A., Jacobsen, S.B., and Boynton, W.V. (1991) Chicxulub crater: a possible Cretaceous/Tertiary boundary impact crater on the Yucatán Peninsula, Mexico. *Geology* 19: 867–871.
- Hode, T., Cady, S.L., von Dalwigk, I., and Kristiansson, P. (2009) Evidence of ancient microbial life in a large impact structure and its Implications for astrobiology: a case study. In *From Fossils to Astrobiology, Records of Life on Earth and Search for Extraterrestrial Biosignature*; edited by J. Seckbach and M. Walsh, Springer Science Series Vol.12 — Cellular Origin, Life in Extreme Habitats and Astrobiology, pp 249–273.
- Iijima, A. (1980) Geology of natural zeolites and zeolitic rocks. *Pure Appl Chem* 52:2115–2130.
- Jeanthon, C., L'Haridon, S., Cuffe, V., Banta, A., Reysenbach, A.-L., and Prieur, D. (2002) *Thermodesulfobacterium hydrogeniphilum* sp. nov., a thermophilic, chemolithoautotrophic, sulfate-reducing bacterium isolated from a deep-sea hydrothermal vent at Guaymas Basin, and emendation of the genus *Thermodesulfobacterium*. *Int J Syst Evol Microbiol* 52: 765–772.
- Kaksonen, A.H., Plumb, J.J., Robertson, W.J., Spring, S., Schumann, P., Franzmann, P.D., and Puhakka, J.A. (2006) Novel thermophilic sulfate-reducing bacteria from a geothermally active underground mine in Japan. *Appl Environ Microbiol* 72:3759–3762.
- Kallmeyer, J., and Boetius, A. (2004) Effects of temperature and pressure on sulfate reduction and anaerobic oxidation of methane in hydrothermal sediments of Guaymas Basin. *Appl Environ Microbiol* 70:1231–1233.

- Kasting, J.F. (2005) Methane and climate during the Precambrian era. *Precambrian Res* 137:119–129.
- Keith, T.E.C., and Staples, L.W. (1985) Zeolites in Eocene basaltic pillow lavas of the Siletz River Volcanics, central Coast Range, Oregon. *Clays Clay Miner* 33:135–144.
- Khelifi, N., Grossi, V., Hamdi, M., Dolla, A., Tholozan, J.-L., Ollivier, B., and Hirschler-Réa, A. (2010) Anaerobic oxidation of fatty acids and alkenes by the hyperthermophilic sulfate-reducing Archaeon *Archaeoglobus fulgidus*. *Appl Environ Microbiol* 76:3057–3060.
- Khelifi, N., Ali, O.A., Roche, Ph., Grossi, V., Brochier-Armanet, C., Valette, O., Ollivier, B., Dolla, A., and Hirschler-Réa, A. (2014) Anaerobic oxidation of long-chain *n*-alkanes by the hyperthermophilic sulfate-reducing archaeon, *Archaeoglobus fulgidus*. *ISME J* 8:2153–2166.
- Koerberl, C. (1993) Chicxulub crater, Yucatan: tektites, impact glasses, and the geochemistry of target rocks and breccias. *Geology* 21:211–214.
- Kohn, M.J., Riciputi, L.R., Stakes, D., and Orange, D.L. (1998) Sulfur isotope variability in biogenic pyrite: reflections of heterogeneous bacterial colonization? *Am Mineral* 83:1454–1468.
- Kring, D.A. (1993) The Chicxulub impact event and possible causes of K/T boundary extinctions. In *Proceedings of the First Annual Symposium of Fossils in Arizona*, edited by D. Boaz and M. Dornan, Mesa Southwest Museum and Southwest Paleontological Society, Mesa, AZ, pp 63–79.
- Kring, D.A. (1995) The dimensions of the Chicxulub impact crater and impact melt sheet. *J Geophys Res* 100:16979–16986.
- Kring, D.A. (2000a) Impact events and their effect on the origin, evolution, and distribution of life. *GSA Today* 10:1–7.
- Kring, D.A. (2000b) Impact-induced hydrothermal activity and potential habitats for thermophilic and hyperthermophilic life. In *Catastrophic Events and Mass Extinctions: Impacts and Beyond*, Lunar and Planetary Institute, Houston, pp 106–107.
- Kring, D.A. (2003) Environmental consequences of impact cratering events as a function of ambient conditions on Earth. *Astrobiology* 3:133–152.
- Kring, D.A. (2005) Hypervelocity collisions into continental crust composed of sediments and an underlying crystalline basement: comparing the Ries (~24 km) and Chicxulub (~180 km) impact craters. *Chemie der Erde* 65:1–46.
- Kring, D.A., and Boynton, W.V. (1992) The petrogenesis of an augite-bearing melt rock in the Chicxulub structure and its relationship to K/T impact spherules in Haiti. *Nature* 358:141–144.
- Kring, D.A., Hildebrand, A.R., and Boynton, W.V. (1991) The petrology of an andesitic melt rock and a polymict breccia from the interior of the Chicxulub structure, Yucatán, Mexico. *Lunar and Planetary Science XXII*, pp 755–756.
- Kring, D.A., Hörz, F., Zurcher, L., and Urrutia-Fucugauchi, J. (2004) Impact lithologies and their emplacement in the Chicxulub impact crater: initial results from the Chicxulub Scientific Drilling Project, Yaxcopoil, Mexico. *Meteorit Planet Sci* 39:879–897.
- Kring, D.A., Schmieder, M., Shaulis, B.J., Riller, U., Cockell, C., Coolen, M.J.L., and the IODP-ICDP Expedition 364 Science Party. (2017a) Probing the impact-generated hydrothermal system in the peak ring of the Chicxulub crater and its potential as a habitat [abstract 1212]. *Lunar and Planetary Science XLVIII*.
- Kring, D.A., Claeys, Ph., Gulick, S.P.S., Morgan, J.V., Collins, G.S., and the IODP-ICDP Expedition 364 Science Party. (2017b) Chicxulub and the exploration of large peak-ring impact craters through scientific drilling. *GSA Today* 27:4–8.
- Kring, D.A., Claeys, Ph., Riller, U., Xiao, L., Collins, G.S., Ferrière, L., Goto, K., Poelchau, M., Rae, A., Tomioka, N., Whalen, M., and the IODP-ICDP Expedition 364 Science Party. (2017c) Emplacing impact melt in the Chicxulub peak ring [abstract 1213]. In *48th Lunar and Planetary Science Conference*, Lunar and Planetary Institute, Houston.
- Kring, D.A., Tikoo, S.M., Schmieder, M., Riller, U., Rebolledo-Vieyra, M., Simpson, S.L., Osinski, G.R., Gattacceca, J., Wittmann, A., Verhagen, C.M., Cockell, C.S., Coolen, M.J.L., Longstaffe, F.J., Gulick, S.P.S., Morgan, J.V., Bralower, T.J., Chenot, E., Christeson, G.L., Claeys, Ph., Ferrière, L., Gebhardt, C., Goto, K., Green, S.L., Jones, H., Lofi, J., Lowery, C.M., Ocampo-Torres, R., Perez-Cruz, L., Pickersgill, A.E., Poelchau, M.H., Rae, A.S.P., Rasmussen, C., Sato, H., Smit, J., Tomioka, N., Urrutia-Fucugauchi, J., Whalen, M.T., Xiao, L., and Yamaguchi, K.E. (2020) Probing the hydrothermal system of the Chicxulub impact crater. *Sci Adv* 6, doi: 10.1126/sciadv.aaz3053.
- Liamleam, W., and Annachatre, A.P. (2007) Electron donors for biological sulfate reduction. *Biotechnol Adv* 25:452–463.
- Liou, J.G. (1971) Analcime equilibria. *Lithos* 4:389–402.
- Lüders, V., and Rickers, K. (2004) Fluid inclusion evidence for impact-related hydrothermal fluid and hydrocarbon migration in Cretaceous sediments of the ICDP-Chicxulub drill core Yaxcopoil-1. *Meteorit Planet Sci* 39:1187–1198.
- Lüders, V., Horsfield, B., Kenkmann, T., Mingram, B., and Wittmann, A. (2003) Hydrocarbons and aqueous fluids in Cretaceous sediments of the ICDP-Chicxulub drill core Yax-1 [abstract 1378]. *Lunar and Planetary Science XXXIV*.
- Machel, H.G. (2001) Bacterial and thermochemical sulphate reduction in diagenetic settings—old and new insights. *Sedimentary Geology* 140:143–175.
- MacLean, L.C.W., Tylliszczak, T., Gilbert, P.U.P.A., Zhou, D., Pray, T.J., Onstott, T.C., and Southam, G. (2008) A high-resolution chemical and structural study of framboidal pyrite formed within a low-temperature bacterial biofilm. *Geobiology* 6:471–480.
- Maher, K.A., and Stevenson, D.J. (1988) Impact frustration of the origin of life. *Nature* 331:612–614.
- Martin, W., Baross, J., Kelley, D., and Russell, M.J. (2008) Hydrothermal vents and the origin of life. *Nat Rev Microbiol* 6:805–814.
- McCarville, P., and Crossey, L.J. (1996) Post-impact hydrothermal alteration of the Manson impact structure. In *The Manson Impact Structure, Iowa*, Special Paper 302, edited by C. Koerberl and R. Anderson, Geological Society of America, Boulder, CO, pp 347–376.
- Mehegan, J.M., Robinson, P.T., and Delaney, J.R. (1982) Secondary mineralization and hydrothermal alteration in the Reydarfjörður drill core, eastern Iceland. *J Geophys Res Solid Earth* 87:6511–6524.
- Mitchell, K., Heyer, A., Canfield, D.E., Hoek, J., and Habicht, K.S. (2009) Temperature effect on the sulfur isotope fractionation during sulfate reduction by two strains of the hyperthermophilic *Archaeoglobus fulgidus*. *Environ Microbiol* 11:2998–3006.
- Mojzsis, S.J., and Harrison, T.M. (2000) Vestiges of a beginning: clues to the emergent biosphere recorded in the oldest known sedimentary rocks. *GSA Today* 10:1–6.
- Morgan, J.V., Gulick, S.P.S., Bralower, T., Chenot, E., Christeson, G., Claeys, Ph., Cockell, C., Collins, G.S., Coolen, M.J.L., Ferrière, L., Gebhardt, C., Goto, K., Jones, H., Kring,

- D.A., Le Ber, E., Lofi, J., Long, X., Lowery, C., Mellett, C., Ocampo-Torres, R., Osinski, G.R., Perez-Cruz, L., Pickersgill, A., Poelchau, M., Rae, A., Rasmussen, C., Rebolledo-Vieyra, M., Riller, U., Sato, H., Schmitt, D.R., Smit, J., Tikoo, S., Tomioka, N., Urutia-Fucugauchi, J., Whalen, M., Wittmann, A., Yamaguchi, K.E., and Zylberman, W. (2016) The formation of peak rings in large impact craters. *Science* 354:878–882.
- Morgan, J., Gulick, S., Mellett, C.L., Green, S.L., and the Expedition 364 Scientists. (2017) *Chicxulub: Drilling the K-Pg Impact Crater*, Proceedings of the International Ocean Discovery Program Vol. 364, International Ocean Discovery Program, College Station, TX.
- Naumov, M.V. (1993) Zeolite mineralization in impact craters [in Russian]. *Zapiski Vsesoyuznogo Mineralogicheskogo Obshchestva* 122:1–12.
- Naumov, M.V. (1996) Basic regularities of the postimpact hydrothermal process. *Solar System Research* 30:21–27.
- Naumov, M.V. (1999) Hydrothermal-metasomatic mineralization [in Russian]. In *Deep Drilling in the Puchezh-Katunki Impact Structure*, edited by V.L. Masaitis and L.A. Pevzner, VSEGEL, St. Petersburg, Russia, pp 276–286.
- Nelson, M.J., Newsom, H.E., Spilde, M.N., and Salge, T. (2012) Petrographic investigation of melt and matrix relationships in Chicxulub crater Yaxcopoil-1 brecciated melt rock and melt rock-bearing suevite (846–885 m, units 4 and 5). *Geochim Cosmochim Acta* 86:1–20.
- Nisbet, E.G., and Sleep, N.H. (2001) The habitat and nature of early life. *Nature* 409:1083–1091.
- Núñez-Cornú, F.J., Prol-Ledesma, R.M., Cupul-Magaña, A., and Suárez-Plascencia, C. (2000) Near shore submarine hydrothermal activity in Bahía Banderas, western Mexico. *Geofísica Internat'l* 39:171–178.
- Nunoura, T., Oida, H., Miyazaki, M., Suzuki, Y., Takai, K., and Horikoshi, K. (2007) *Desulfothermus okinawensis* sp. nov., a thermophilic and heterotrophic sulfate-reducing bacterium isolated from a deep-sea hydrothermal field. *Int J Syst Evol Microbiol* 57:2360–2364.
- Pace, N.R. (1991) Origin of life—facing up to the physical setting. *Cell* 65:531–533.
- Pace, N.R. (1997) A molecular view of microbial diversity and the biosphere. *Science* 276:734–740.
- Parnell, J., Boyce, A., Thackeray, S., Muirhead, D., Lindgren, P., Mason, C., Taylor, C., Still, J., Bowden, S., Osinski, G.R., and Lee, P. (2010) Sulfur isotope signatures for rapid colonization of an impact crater by thermophilic microbes. *Geology* 38:271–274.
- Peter, J.M., and Shanks, W.C., III (1992) Sulfur, carbon, and oxygen isotope variations in submarine hydrothermal deposits of Guaymas Basin, Gulf of California, USA. *Geochim Cosmochim Acta* 56:2025–2040.
- Popa, R., Kinkle, B.K., and Badescu, A. (2004) Pyrite framboids as biomarkers for iron-sulfide systems. *Geomicrobiol J* 21:193–206.
- Prol-Ledesma, R.M., Canet, C., Melgarejo, J.C., Tolson, G., Rubio-Ramos, M.A., Cruz-Ocampo, J.C., Ortega-Osorio, A., Torres-Vera, M.A., and Reyes, A. (2002) Cinnabar deposition in submarine coastal hydrothermal vents, Pacific margin of central Mexico. *Econ Geol* 97:1331–1340.
- Reysenbach, A.-L., and Shock, E. (2002) Merging genomes with geochemistry in hydrothermal ecosystems. *Science* 296:1077–1082.
- Roerdink, D.L., Mason, P.R.D., Whitehouse, M.J., and Reimer, T. (2013) High-resolution quadruple sulfur isotope analyses of 3.2 Ga pyrite from the Barberton Greenstone Belt in South Africa reveal distinct environmental controls on sulfide isotopic arrays. *Geochim Cosmochim Acta* 117:203–215.
- Roerdink, D.L., Mason, P.R.D., Whitehouse, M.J., and Brouwer, F.M. (2016) Reworking of atmospheric sulfur in a Paleoproterozoic hydrothermal system at Londozi, Barberton Greenstone Belt, Swaziland. *Precambrian Res* 280:195–204.
- Rowe, A.J., Wilkinson, J.J., Coles, B.J., and Morgan, J.V. (2004) Chicxulub: testing for post-impact hydrothermal input into the Tertiary ocean. *Meteorit Planet Sci* 39:1223–1231.
- Russell, M.J. and Arndt, N.T. (2005) Geodynamic and metabolic cycles in the Hadean. *Biogeosciences* 2:97–111.
- Schaefer, B., Grice, K., Coolen, M.J.L., Summons, R.E., Cui, X., Bauersachs, T., Schwark, L., Böttcher, M.E., Bralower, T.J., Lyons, S.L., Freeman, K.H., Cockell, C.S., Gulick, S.P.S., Morgan, J.V., Whalen, M.T., Lowery, C.M., and Vajda, V. (2020) Microbial life in the nascent Chicxulub crater. *Geology* 48:328–332.
- Schmieder, M., Kring, D.A., Goderis, S., Claeys, Ph., Coolen, M.J.L., and Wittmann, A. (2017a) Secondary sulfides in hydrothermally altered impactites and basement rocks of the Chicxulub peak ring—a preliminary survey [abstract 6139]. In *80th Annual Meeting of the Meteoritical Society*, Lunar and Planetary Institute, Houston.
- Schmieder, M., Kring, D.A., and the IODP-ICDP Expedition 364 Science Party. (2017b) Petrology of target dolerite in the Chicxulub peak ring and a possible source of K/Pg boundary picotite spinel [abstract 1235]. *Lunar and Planetary Science XLVIII*.
- Schmieder, M., Ross, D.K., Robinson, K.L., and Kring, D.A. (2019) Titanium-in-quartz geothermometry of impactites and peak-ring lithologies from the Chicxulub impact crater [abstract 2132]. *Lunar and Planetary Science L*.
- Schulte, M., Blake, D., Hoehler, T., and McCollom, T. (2006) Serpentinization and its implications for life on the early Earth and Mars. *Astrobiology* 6:364–376.
- Schwartzman, D.W., and Lineweaver, C.H. (2004) The hyperthermophilic origin of life revisited. *Biochem Soc Trans* 32:168–171.
- Sharpton, V.L., Marín, L.E., Carney, J.L., Scott, L., Ryder, G., Schuraytz, B.C., Sikora, P., and Spudis, P.D. (1996) A model of the Chicxulub impact basin based on an evaluation of geophysical data, well logs, and drill core samples. In *The Cretaceous-Tertiary Event and Other Catastrophes in Earth History*, Special Paper 307, edited by G. Ryder, D. Fastovsky, and S. Gartner, Geological Society of America, Boulder, CO, pp 55–74.
- Shen, Y., and Buick, R. (2004) The antiquity of microbial sulfate reduction. *Earth-Science Reviews* 64:243–272.
- Shen, Y., Buick, R., and Canfield, D.E. (2001) Isotopic evidence for microbial sulphate reduction in early Archaean era. *Nature* 410:77–81.
- Shibuya, T., Russell, M.J., and Takai, K. (2016) Free energy distribution and hydrothermal mineral precipitation in Hadean submarine alkaline vent systems: importance of iron redox reactions under anoxic conditions. *Geochim Cosmochim Acta* 175:1–19.
- Shock, E.L., and Schulte, M.D. (1998) Organic synthesis during fluid mixing in hydrothermal systems. *J Geophys Res* 103:28513–28527.
- Sim, M.S., Bosak, T., and Ono, S. (2011) Large sulfur isotope fractionation does not require disproportionation. *Science* 333:74–77.
- Simpson, S.L., Boyce, A.J., Lambert, P., Lindgren, P., and Lee, M.R. (2017) Evidence for an impact-induced biosphere from

- the $\delta^{34}\text{S}$ signature of sulphides in the Rochechouart impact structure, France. *Earth Planet Sci Lett* 460:192–200.
- Simpson, S.L., Osinski, G.R., Longstaffe, F.J., Schmieder, M., and Kring, D.A. (2020) Hydrothermal alteration associated with the Chicxulub impact crater upper peak-ring breccias. *Earth Planet Sci Lett* 547, doi:10.1016/j.epsl.2020.116425.
- Sleep, N.H., Zahnle, K.J., Kasting, J.F., and Morowitz, H.J. (1989) Annihilation of ecosystems by large asteroid impacts on the early Earth. *Nature* 342:139–142.
- Smith, R.L., and Klug, M. (1981) Electron donors utilized by sulfate-reducing bacteria in eutrophic lake sediments. *Appl Environ Microbiol* 42:116–121.
- Stetter, K.O., Lauerer, G., Thomm, M., and Neuner, A. (1987) Isolation of extremely thermophilic sulfate reducers: evidence for a novel branch of archaeobacteria. *Science* 236:822–824.
- Stockbridge, R.B., Lewis, C.A., Jr., Yuan, Y., and Wolfenden, R. (2010) Impact of temperature on the time required for the establishment of primordial biochemistry, and for the evolution of enzymes. *Proc Natl Acad Sci USA* 107:22102–22015.
- Strauss, H., and Deutsch, A. (2003) The Chicxulub event—sulfur-bearing minerals and lithologies. *Gophysical Research Abstracts* 5:04905.
- Ueda, S., Murata, H., Koizumi, M., and Nishimura, H. (1980) Crystallization of mordenite from aqueous solutions. *Am Mineral* 65:1012–1019.
- Utada, M. (2001) Zeolites in hydrothermally altered rocks. *Rev Mineral Geochem* 45:305–322.
- Westall, F., Hickman-Lewis, K., Hinman, N., Gautret, P., Campbell, K.A., Br  h  ret, J.G., Foucher, F., Hubert, A., Sorieul, S., Dass, A.V., Kee, T.P., Georgelin, T., and Brack, A. (2018) A hydrothermal-sedimentary context for the origin of life. *Astrobiology* 18:259–293.
- Whitehouse, M.J. (2013) Multiple sulfur isotope determination by SIMS: evaluation of reference sulfides for $\Delta^{33}\text{S}$ with observations and a case study on the determination of $\Delta^{36}\text{S}$. *Geostandards and Geoanalytical Research* 37:19–33.
- Whitehouse, M.J., and Fedo, C.M. (2007) Searching for Earth's earliest life in southern West Greenland—history, current status, and future prospects. In *Earth's Oldest Rocks, Developments in Precambrian Geology*, Vol. 15, edited by M.J. Van Kranendonk, R.H. Smithies, and V. Bennett, Elsevier, Amsterdam, pp 841–853.
- Wilkin, R. and Barnes, H. (1997) Formation processes of framboidal pyrite. *Geochim Cosmochim Acta* 61:323–339.
- Woese, C.R., Kandler, O., and Wheelis, M.L. (1990) Towards a natural system of organisms: proposal for the domains Archaea, Bacteria, and Eucarya. *Proc Natl Acad Sci USA* 87:4576–4579.
- Wolfenden, R., Lewis, C.A., Jr., Yuan, Y., and Carter, C.W., Jr. (2015) Temperature dependence of amino acid hydrophobicities. *Proc Natl Acad Sci USA* 112:7484–7488.
- Zahnle, K.J., Arndt, N., Cockell, C., Halliday, A., Nisbet, E., Selsis, F., and Sleep, N.H. (2007) Emergence of a habitable planet. *Space Sci Rev* 129:35–78.
- Zahnle, K.J., Lupo, R., Catling, D.C., and Wogan, N. (2020) Creation and evolution of impact-generated reduced atmospheres of early Earth. *Planet Sci J* 1, doi:10.3847/PSJ/ab7e2c.
- Z  rcher, L., and Kring, D.A. (2004) Hydrothermal alteration in the core of the Yaxcopoil-1 borehole, Chicxulub impact structure, Mexico. *Meteorit Planet Sci* 39:1199–1221.
- Zurcher, L., Kring, D.A., Barton, M.D., Dettman, D., and Rollog, M. (2005) Stable isotope record of postimpact fluid activity in the core of the Yaxcopoil-1 borehole, Chicxulub impact structure, Mexico. In *Large Meteorite Impacts III*, Special Paper 384, edited by T. Kenkmann, F. H  rz, and A. Deutsch, Geological Society of America, Boulder, CO, pp 223–238.

Address correspondence to:

David A. Kring
Lunar and Planetary Institute
Universities Space Research Association
3600 Bay Area Blvd.
Houston, TX 77058-1113
USA

E-mail: kring@lpi.usra.edu

Submitted 28 April 2020

Accepted 14 October 2020

Associate Editor: Tim Lyons

Abbreviations Used

- ICDP = International Continental Scientific Drilling Program
IODP = International Ocean Discovery Program
mbsf = meters below the seafloor
V-CDT = reference value for Vienna Canyon Diablo Troilite
V-PDB = reference value for Vienna Pee Dee Belemnite
Y-6 = Yucat  n-6
Yax-1 = Yaxcopoil-1